Journal of Petroleum Science and Engineering 163 (2018) 661–670

Contents lists available at ScienceDirect

Journal of Petroleum Science and Engineering

journal homepage: www.elsevier.com/locate/petrol

Implications for improved polymer gel conformance control during low-salinity chase-floods in fractured carbonates

B. Brattekås [a,*], R.S. Seright [b,1]

[a] The National IOR Centre of Norway, Dept. of Petroleum Technology, University of Stavanger, Norway
[b] Petroleum Recovery Research Centre, New Mexico Institute of Mining and Technology, NM, USA

ARTICLE INFO

Keywords:
Polymer gel
Low-salinity chase-flooding
Improved blocking capacity
Fractured carbonates
Influence of oil
PET imaging

ABSTRACT

Polymer gel is often used to reduce flow through highly conductive fracture networks, frequently present in naturally fractured carbonate reservoirs. When in place, polymer gel efficiently reduces fracture flow and may improve sweep efficiency and oil recovery during water chase-floods. Polymer gel treatments have in some cases been less efficient than expected in reducing fracture conductivity. This may occur because the polymer gel only partially fills the fracture volume, and allows fracture channeling of injected fluids. Low-salinity waterfloods may improve polymer gel blocking of fractures and remedy less efficient polymer gel treatments. Previous experimental work has shown that low-salinity waterfloods, where the salinity is reduced with respect to the gel solvent, reduces fracture channeling and restores matrix flow. This work further investigates low-salinity waterflooding as a method to improve conformance during polymer gel treatments in fractured, low permeable, carbonate rock. The low flow capacity of carbonate may cause a less efficient gel blocking of fractures, although the gel behaves according to established models during injection. Low-permeable carbonate core plugs with open, highly conductive fractures were used for this study. Water flow paths during high-salinity and low-salinity waterflooding were evaluated by positron emission tomography (PET). We found that gel blocking efficiency during chase waterfloods depends on: 1) the salinity of the chase water. Gel blocking efficiency increases with low-salinity water throughput; opposite to high-salinity waterfloods, where the gel blocking is reduced with water throughput. 2) The core material. As expected, a higher pressure was required to maintain flow through the matrix during water chase-floods in low-permeable carbonates. Water was diverted into the matrix for all ranges of permeability: sandstone and low-permeable carbonates, during low-salinity waterfloods. 3) The presence of oil. Fracture channeling prevailed during low-salinity waterfloods in chalk cores with residual oil present.

1. Introduction

Polymer gel may be used for a range of applications within medicine (e.g. dosimetry, sustained-release drug systems), the consumer industry (contact lenses, disposable diapers, clothing etc.) and also in the oil and gas industry. An important objective of polymer gel applications in petroleum reservoirs is to reduce fracture conductivity and enable matrix flow. Gels are often used in watered-out wells to limit high water cuts, but may also be used to reduce fracture conductivity and improve sweep efficiency in-depth, which may improve oil recovery. The water content of a polymer gel is high, often above 99%, with the remaining <1% consisting of polymer molecules and a cross-linking agent. Polymers may be used for Enhanced Oil Recovery (EOR) purposes alone, to increase the viscosity of the water phase and improve mobility during water-oil displacement within a rock matrix. When conductive fractures are present, however, injected fluids will often flow through the fracture network, without entering the matrix to displace oil. A cross-linker may be added to the polymer solution, which is then termed a *gelant*: when the gelant is exposed to an elevated temperature for a period of time known as the gelation time, the polymer molecules bond together and form a three-dimensional polymer gel network. Formed polymer gel has a significant viscosity and is an efficient fracture blocker. During injection, formed gel does not enter into porous rock (R.S. Seright, 2001) hence gel flow is restricted to the fracture network. Dehydration of the polymer gel network is expected to occur during gel propagation through fractures, investigated in several publications by Seright (e.g. (R.S. Seright, 2001, 2003a,b)). Dehydration, also termed "leakoff", is a process where water leaves the gel, which causes the polymer gel to concentrate and become

* Corresponding author. Visiting address: Allègaten 55, 5007 Bergen, Norway.
E-mail addresses: bergit.brattekas@uib.no (B. Brattekås), randy.seright@nmt.edu (R.S. Seright).
[1] Address: PRRC, 801 Leroy Place, 87801 Socorro, New Mexico, USA.

https://doi.org/10.1016/j.petrol.2017.10.033
Received 23 June 2017; Received in revised form 3 October 2017; Accepted 11 October 2017
Available online 12 October 2017
0920-4105/

more rigid. The dehydrated and concentrated gel forms a filter cake in the fracture, which is highly resistant towards pressure during chase-floods. Water may flow through the matrix during leakoff, or channel through the fracture network ahead of the gel. During continuous gel injection, fresh gel flows through the dehydrated gel filter cake in designated flow channels termed *wormholes* (Brattekås et al., 2017; R.S. Seright, 2003a,b). With gel in place in fractures, injected fluids may enter into matrix blocks during chase floods, to displace oil.

Several occurrences may cause the polymer gel treatment to be less efficient; i.e. changes occur in the polymer gel that may open parts of the fracture volume to flow. These include syneresis (Romero-Zeron et al., 2008) loss of cross-linker to the formation by diffusion (Ganguly et al., 2002; Wilton and Asghari, 2007) or loss of solvent to the formation by capillary spontaneous imbibition (Brattekås et al., 2014). Mechanical degradation of the gel may also occur at elevated injection pressures: gel of injected composition, residing in the wormholes, is displaced from the fracture at *the gel rupture pressure* (Brattekås et al., 2015; Ganguly et al., 2002; R. S. Seright, 2003b). When parts of the fracture volume is re-opened to flow, injected fluids may resume channeling through the fracture network, which results in decreased sweep efficiency and oil recovery. The volume of gel residing in a fracture controls conformance improvement in fractured reservoirs, by opening or closing parts of the fracture to flow. Changes in external conditions around a polymer gel network, e.g. changes in temperature, solvent composition, ionic strength and external electric field (Horkay et al., 2000), may also alter the gel volume and impact the blocking capacity of gel residing in a fracture. The effects of salinity contrasts on gel swelling and shrinking behavior have often been demonstrated in experiments using pre-formed particle gel (PPG), showing different gel swelling behavior in brines of different salinity (Bai et al., 2007; Zhang and Bai, 2011) or bulk volumes of gel, indicating that volumetric changes in the gel volume may occur if the salinity of the contacting aqueous phase differs from the gel solvent (Aalaie et al., 2009; Tu and Wisup, 2011).

Improved polymer gel fracture blocking was recently demonstrated during low-salinity waterfloods (Brattekås et al., 2016): high-salinity polymer gel was placed in a fracture and the salinity of the water was reduced with respect to the gel solvent during chase-floods. Improved gel blocking during low-salinity waterflooding was observed by an increase in injection pressure and matrix production. In some cores the injection pressure increased to above the original rupture pressure and the fracture was completely blocked by gel, hence all injected fluids were diverted into the matrix. The experiments were performed using sandstone and limestone (carbonate) core plugs.

In the current work, low-salinity chase-floods of polymer gel treated fractures through low-permeable carbonate core plugs with residual oil saturations are presented. To maintain a given flow rate, a higher pressure gradient is required to flood low-permeable rock matrix during chase-floods compared to high-permeability rock (e.g., carbonate versus sandstone) d. Presence of oil also influences the ease of which water flows through the porous rock, because the relative permeability of water is decreased. The typically fractured nature of carbonate reservoirs produce a high permeability ratio between fractures (thousands of Darcy) and the low-permeable matrix (frequently millidarcy (mD) scale), where the flow pattern during and after gel placement may be challenging to determine. Several publications based in experimental work suggest that placement of formed gel behaves according to established models as long as the flow capacity of the core material adjacent to the fracture exceeds that of the very low-permeable polymer gel (Liang et al., 1993; R.S. Seright, 2003a; R. S. Seright and Martin, 1993). Rock properties were not observed to influence the gel tolerance for pressure during chase-floods, estimated by measuring the rupture pressure (Brattekås et al., 2015). Basic flow equations(e.g. the Darcy equation), however, dictate that fluid flow through rock matrix is highly dependent on rock properties and, thus, the core material, where the water flow rate is controlled by matrix permeability, saturation functions (relative permeability and capillary pressure) and injection pressure. Thus; rock properties will influence flow patterns during chase-floods even though they are not expected to influence the polymer gel placed in the fracture. We propose that the fluid flow pattern through fractured cores with very low permeability is affected by the flow capacity of the matrix (essentially controlled by the relative permeability to water in these experiments) compared to the fracture conductivity to water. Experiments were performed to investigate the effects of low-salinity flooding on gel blocking capacity and oil recovery in fractured chalk and limestone cores of low matrix permeability. Our current work examines gel effectiveness for diversion in fractured cores (1) with and without oil present, (2) in sandstone, chalk, and limestone cores with a range of permeability, and (3) using high-and low-salinity chase waters. PET experiments were useful for visualizing important mechanisms of diversion associated with the gel.

2. Experimental methods and materials

An overview of the experiments and core properties are provided in Table 1. Cylindrical core plugs were drilled out from larger blocks of Rørdal chalk (Ekdale and Bromley, 1993) or Edwards limestone (Tie, 2006). Core 3 was sawed out from a large chalk block to facilitate a longer fracture, and was rectangular. Absolute permeability is in the range of 1-10mD for Rørdal chalk (frequently in the range of 3-6mD, $\phi = 42–46\%$), and 3-28mD for the Edwards limestone ($\phi = 16–26\%$). The chalk core material is expected to be homogeneous, while the limestone was shown to have a trimodal pore size distribution, exhibiting both microscopic pores and macroscopic vugs (Riskedal et al., 2008). A Bentheimer sandstone core plug (Klein and Reuschle, 2003) was used in this work for comparison purposes. All core materials were outcrops, and expected to be strongly water-wet (Viksund et al., 1998). Longitudinal fractures through the cores were created using a band saw. The cores were re-assembled with a POM (Polyoxymethylene) spacer between the matrix halves to keep the fracture open and maintain a constant fracture aperture of 1 mm. The outer core circumferences were covered in epoxy resin to prevent flow. Specially designed end pieces with three flow ports-one for the fracture and one for each matrix half-was used for all core outlets. This allowed separate measurements of matrix and fracture production. The fracture surfaces were left open to flow in all experiments. Two different core setups were used, shown in Fig. 1: For cores 1–6 (Fig. 1, ***Left***), POM end pieces were glued to the core inlets, which facilitated a common inlet for the fracture and two matrix core halves. For Core 7 (Fig. 1, ***Right***), the specially designed end piece with three flow ports-one for the fracture and one for each matrix half-was also used for the inlet, to allow chase water injection directly into the matrix. The flow paths during high- and low-salinity chase-floods were visualized by PET. The core and experimental setup is schematically represented in Fig. 1.

2.1. Experimental schedule

The experimental schedule was the same for all cores:

2.1.1. Preparations

1) Saturation under vacuum, either by high-salinity brine (Core 1 only-4 wt% NaCl, 3.4 wt% $MgCl_2*6H_2O$, 0.5 wt% $CaCl_2*2H_2O$) or mineral oil (n-Decane).
2) 0.5% HPAM polymer (~5 million Daltons molecular weight) was mixed in high-salinity brine, 0.0417 wt% (417 ppm) Cr(III)-acetate was added, and the gelant solution was aged at T = 41 °C for 24 h to form polymer gel. The gel was cooled to ambient conditions before injection. Because the gel was pre-formed, it is contained to the longitudinal fracture during injection (R.S. Seright, 2001). Leakoff water may leave the gel and progress through the matrix.

2.1.2. Core flooding schedule

Inlet pressures were measured in all experiments, during the core

Table 1
Overview of core plugs and type of fluid used during chase-floods.

Core ID		Length [cm]	Diameter [cm]	Rupture pressure [kPa/cm]	Chase-flood	Saturation (at chase-flood start)
Core 1	Chalk	6.04	5.07	7.5	High-salinity water	100% water
Core 2	Chalk	8.63	3.79	8.8	High-salinity water	Residual oil
Core 3	Chalk	19.80	2.42[a]	2.6	High-salinity and low-salinity water	Residual oil
Core 4	Sandstone	6.94	5.15	5.0	Low-salinity water	Residual oil
Core 5	Limestone	14.74	4.89	4.5	Low-salinity water	Residual oil
Core 6	Chalk	8.62	3.79	9.0	Low-salinity water	Residual oil
Core 7	Limestone	7.56	4.96	4.4	High-salinity and low-salinity water	Residual oil

[a] Core 3 was rectangular.

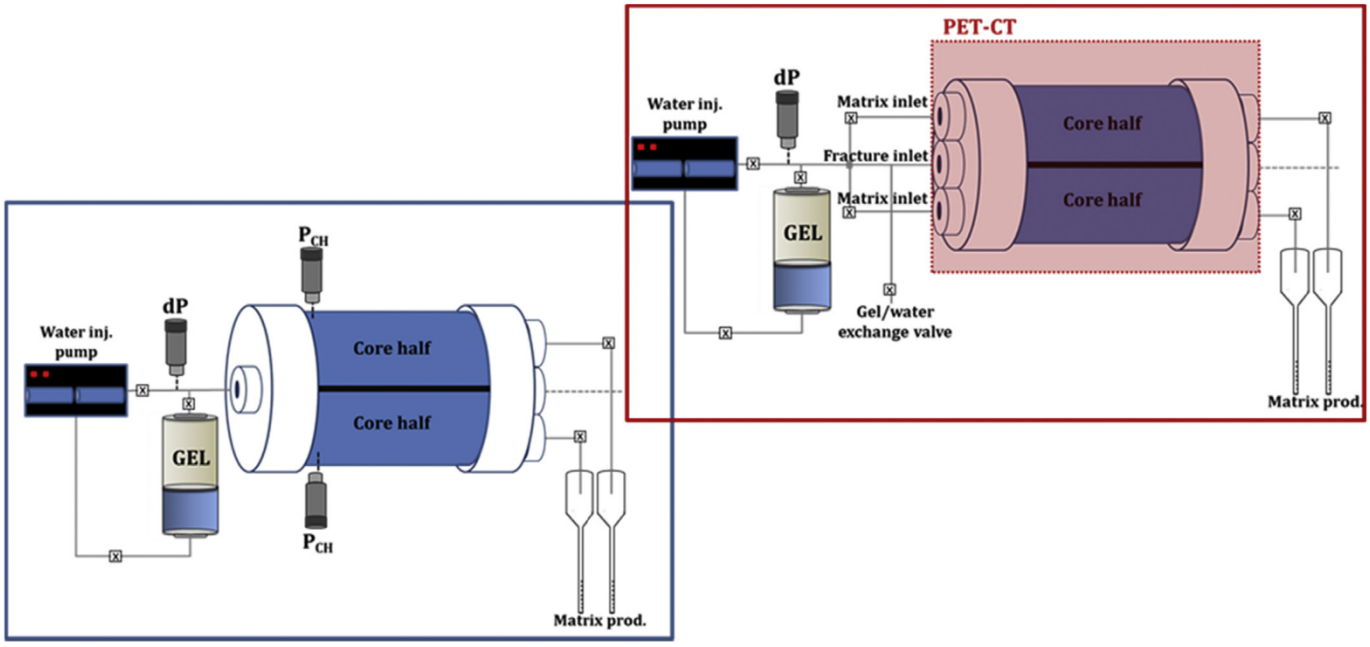

Fig. 1. Setups used in the experiments. **Left:** Experimental setup used during preflush, gel placement and chase waterflooding of cores 1 to 6. All fluids were injected into one common inlet. **Right:** Experimental setup for Core 7, placed in a small-animal PET-CT scanner during high-salinity and low-salinity chase waterfloods.

flood schedule. In Core 1–6, matrix pressures were also measured, and fluid production was measured for each matrix half and the fracture separately. In Core 7, fluid flow paths were qualitatively investigated using a PET-CT scanner. The schedule for core flooding was:

3) Injection of saturation fluid. Water (for Core 1) or oil (for Cores 2–7) was injected to measure the average flow capacity of the fractured core plugs. Matrix conductivity was measured by fluid injection into the matrix at several flow rates, keeping the fracture outlet closed, and confirmed that the core permeability was in accordance with references values. When both matrix and fracture outlets were open, virtually all fluid flow occurred through the fracture. Several flow rates were used to confirm this and verify fracture conductivity. (Due to the fixed fracture aperture, fracture conductivity was assumed to be the same for all core plugs, and calculated using the cubic law of Witherspoon et al. (1980)).
4) Polymer gel injection at a constant rate of 200 mL/h for 4 h. This gel volume (800 cm^3) corresponds to several pore volumes for each core. Formed gel propagated through the fracture without entering into the matrix. Water leaked off into the matrix halves due to gel dehydration and was measured volumetrically versus time through the matrix production outlets. Initially, oil was displaced from the matrix and produced through the matrix production outlets. Some oil was also displaced through the fracture and accumulated in the produced gel; this oil was not quantifiable. Oil production through the matrix production outlets ceased in Cores 2 to 7 within 2 h of gel injection. At this point, the matrix oil saturation was below 40%, i.e. more than 60% of the oil originally in place (OOIP) was produced through the matrix production outlets. For the given core materials at strongly water-wet conditions, this corresponds to the residual oil saturation (Viksund et al., 1998). Viscosity measurements of the matrix effluent confirmed that water alone was produced from the matrix after this time.
5) Chase-flooding by high-salinity brine (4 wt% NaCl, 3.4 wt% $MgCl_2$*$6H_2O$, 0.5 wt% $CaCl_2$*$2H_2O$) and/or low-salinity water (distilled water). Water flow rates varied between experiments during high-salinity waterflooding; the flow rate was initially low at 6 mL/h to accurately measure the gel rupture pressure. After rupture, the flow rate was stepwise increased to test the gel blocking efficiency. Low-salinity waterflooding was performed using a continuous low flow rate of 6 mL/h. A low flow rate was necessary during PET imaging, for controlled investigation of the changing flow pattern during low-salinity waterflooding, and was used in all cores to render the result comparable.

3. Results and discussion

3.1. Baseline study: high-salinity chase-flood

To discuss low-salinity chase-floods, a baseline must first be established that describe gel blocking ability during high-salinity chase-floods. In Core 1 (fully water saturated) and Core 2 (initially fully oil saturated), the chase water salinity was equal to that of the gel solvent. Fig. 2 shows experimental measurements of injection pressure, matrix pressures and

matrix/fracture fluid production during pre-flood, gel placement and water chase-flood into the two fractured chalk core plugs. Due to the core setup (Fig. 1, ***Left***), all fluids were injected into a common inlet for the fracture and matrix core halves. Pre-floods were performed using the saturating fluid-water for Core 1 and oil for Core 2. The open fracture has a permeability in the range of $8.4*10^7$D (calculated using the law of Witherspoon et al. (1980)). All fluids flowed through the fracture during pre-floods, and no pressure buildup was detected in the matrix. Polymer gel was injected to reduce fracture conductivity. The specially-designed end piece at the outlet accommodated measurement of matrix and fracture production separately. Gel was only produced through the fracture outlet in both cores. In Core 1, water only was produced through the matrix outlets during gel injection. In Core 2, oil was produced through the matrix for approximately 2 h, during which the oil saturation was reduced to the residual oil saturation. Water was produced alongside oil after breakthrough, and alone for the last 2 h of gel injection. Chase waterfloods were performed, using high-salinity water. The gel remained intact in the fracture during low rate waterflooding of Core 1, and all injected fluids were produced through the matrix outlets (Fig. 2, ***Top***). In Core 2, with residual oil present, fluid production from the matrix was initially low, and only 30% of the total fluid production was from the matrix. Gel rupture occurred at a low injection rate of 6 mL/h in Core 2 (gel rupture is characterized by a sudden drop in pressure corresponding with increased fluid production from the fracture outlet), after which fluid production from the matrix quickly decreased to 5% of the total production. In Core 1, gel rupture was forced by increasing the injection rate in several steps. After gel rupture, matrix production quickly decreased to 10% of the total flow rate, twice as high as the Core 2 matrix production. The low matrix production rate from Core 2 was caused by the low relative permeability to water in the matrix; thus, an elevated pressure gradient is required for matrix flow compared to Core 1.

3.2. Low-salinity chase-flood

Low-salinity waterflooding provides a possibility to increase the gel strength and improve fracture blocking efficiency during chase-floods (Brattekås et al., 2016). In this work, low-salinity waterflooding was performed in fractured, low-permeable carbonate cores, after gel placement and, in some cores, following a high-salinity waterflood. Chalk Core 3 was used to test the potential for low-salinity flooding in fractured chalk. Core 3 was initially oil saturated; during gel placement, leakoff water flooded into the matrix to displaced oil, and the oil saturation was reduced to the residual oil saturation. Fig. 3 illustrates high-salinity waterflooding with following low-salinity waterflooding into Core 3, and the results are compared to Core 2 (high-salinity waterflooding only). The waterfloods were both performed using low injection rates of 6 mL/h. Because the duration of the two experiments varied significantly-from 2 h of high-salinity waterflooding into Core 2, to 119 h of high-salinity and low-salinity waterflooding into Core 3. Time (x-axis in Fig. 3) was normalized with respect to the total duration of

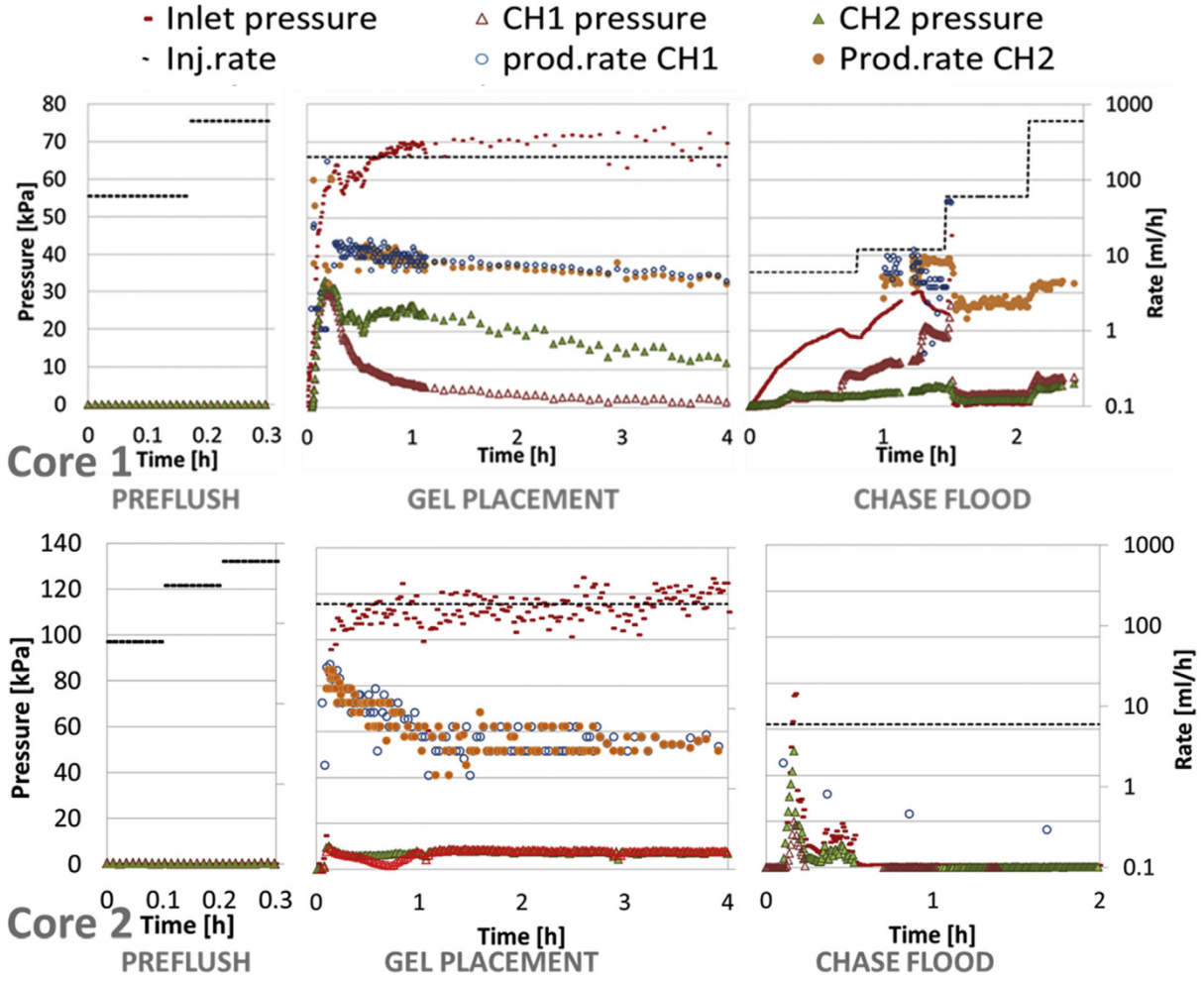

Fig. 2. Preflush, gel placement and high-salinity water chase-flooding into **Top:** a fully water saturated chalk core (Core 1). The gel did not rupture during waterflooding at low rates, and the matrix flow rate remained high. **Bottom:** a chalk core with a residual oil saturation (Core 2) and thus decreased water relative permeability. Matrix production swiftly decreased to below 10% of the total flow rate, and water was forced to flow through the fracture. No clear rupture pressure was achieved during waterflooding. The term "CH" is an abbreviation for "Core Half".

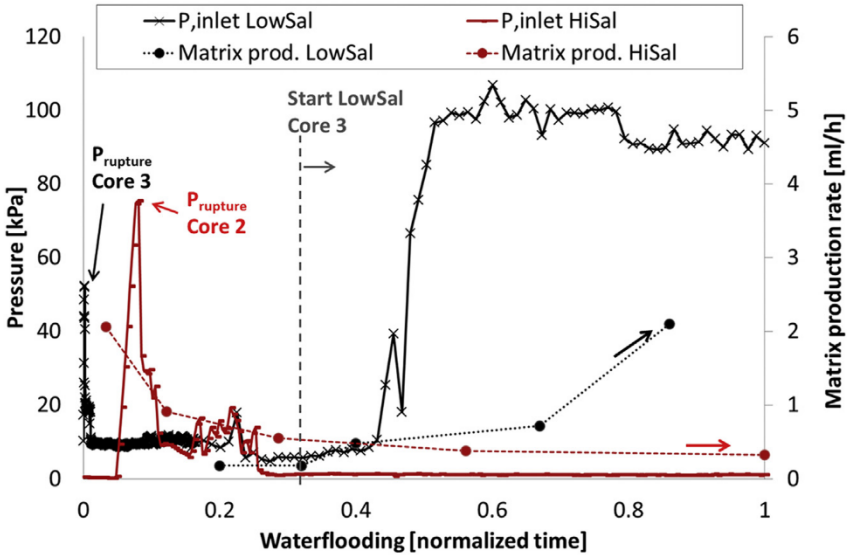

Fig. 3. Water chase-flooding of chalk cores with oil present: high-salinity (Core 2) compared to low-salinity (Core 3) waterflooding. The injection pressure and matrix production rate increase during low-salinity waterflooding, indicating improved gel blocking.

waterflooding for both cores. The pressure trends during high-salinity flooding were comparable in both cores. The gel blocking efficiency during high-salinity waterflooding of Core 2 and Core 3 quickly decreased, as measured by the injection pressure and separate water production from the matrix and fracture outlets. The rupture pressures were immediately reached during high-salinity water injection, after which injection pressures swiftly decreased and stabilized at lower levels. Although the pressure trends were fairly stable after gel rupture, the gel blocking efficiency continued to decrease with water throughput-this is expected behavior caused by erosion of the gel (Brattekås et al., 2015). Water flow through the matrix production outlets constituted 5% of the total production after 2 h of waterflooding for Core 2 and 3% after 22 h for Core 3. The low matrix production indicates that the relative permeability of water in the matrix yields a lower flow capacity than that in the partially gel-filled fracture. Low-salinity waterflooding was initiated in Core 3 at this time (normalized time t = 0.32, marked by a grey line in Fig. 3). The injection pressure did not immediately respond to the salinity change, and an induction period of 22.7 h was observed before the pressure started increasing. Although changes in pressure were not observed, fluid production from the matrix increased by 5% during the first 2.5 h of low-salinity waterflooding, and 8% of injected fluids were produced through the matrix. This indicates a change towards improved gel blocking, where a higher fraction of injected water is diverted into the matrix. When low-salinity waterflooding progressed for 54 h (corresponding to normalized time 0.56), the pressure increased to, and stabilized at, a level almost twice as high as the initial rupture pressure. Increased matrix production was also measured, at 12%, from 69.5 to 72 h of low-salinity waterflooding (corresponding to normalized time 0.67–0.69), and 35% during late-stage waterflooding (95–97 h of low-salinity injection, at normalized time 0.98–1). The increase in pressure and matrix production is caused by improved gel fracture blocking during low-salinity waterfloods. Water diversion was improved with water throughput, which is opposite to how gel behaves during high-salinity waterfloods.

When fluid production from the matrix increased, an unexpected effect of low-salinity waterflooding was observed, and oil was produced from the matrix and fracture outlets. A slow production of oil continued throughout the entire stable pressure period (from t = 54 h of low-salinity water injection), totaling 3.4% of the oil originally in place (OOIP). The rock used in this study was expected to be strongly water-wet, and enhanced oil recovery owing to a change in wettability (Morrow and Buckley, 2011) is therefore not likely. It is, however, likely that oil production was observed in Core 3 due to the core shape. Core 3 was rectangular and longer than the other cores, and the pressure gradient during oil displacement by leakoff water points from the fracture (where the gel is) into the matrix. The displacement of oil from the matrix occurs until water established a continuous path between the fracture and outlet location. At this point, oil may be trapped behind the water front, e.g. in the corners of Core 3. During waterflooding, the direction of the pressure changes, and points from the inlet towards the outlet. Improved sweep by low-salinity waterflooding may therefore recover previously trapped oil, by establishing new flow paths in the matrix. Production of oil was not observed during low-salinity floods in the remaining cores.

3.3. Effect of core material

Low-salinity chase-floods were tested in three different, fractured core materials: sandstone (Core 4), limestone (Core 5) and chalk (Core 6). High-salinity water was first injected to rupture the gel, after which the water was changed to low-salinity water and the cores flooded at a low rate of 6 mL/h for a prolonged period of time. The results from low-salinity flooding are shown in Fig. 4. The duration of low-salinity waterflooding was 234 h for Core 4, 1023 h for Core 5 and 49 h for Core 6; the x-axis of Fig. 4 was normalized with respect to the low salinity flooding time for each core plug, for improved comparison of the data. Fig. 4 ***(Left)*** shows the measured injection pressure for each core plug: the injection pressure swiftly increased in each of the core plugs when low-salinity waterflooding was initiated, which suggests improved fracture blocking by gel. The measured injection pressures were different during early stage low-salinity waterflooding, however; after significant throughput of low-salinity water, similar pressure values were observed for all three cores (marked "Region 1" in the figure). The permeability ratio between the three core plugs may be as high as 1000 (between sandstone and chalk), and the pore size variation is equivalently large. Similar injection pressures for the three vastly different core materials therefore indicate that the pressure is largely controlled by the gel in these experiments. Specifically, gel residing in the inlet end pieces represent a flow barrier for fluids to enter the matrix. The volume and strength of this gel barrier is comparable for all experiments, due to the use of duplicated end pieces.

Fig. 4 ***(Right)*** shows the measured matrix pressures and matrix production for the three core plugs during low-salinity waterflooding. Matrix production (second y-axis) is given as a fraction of the injected rate. As

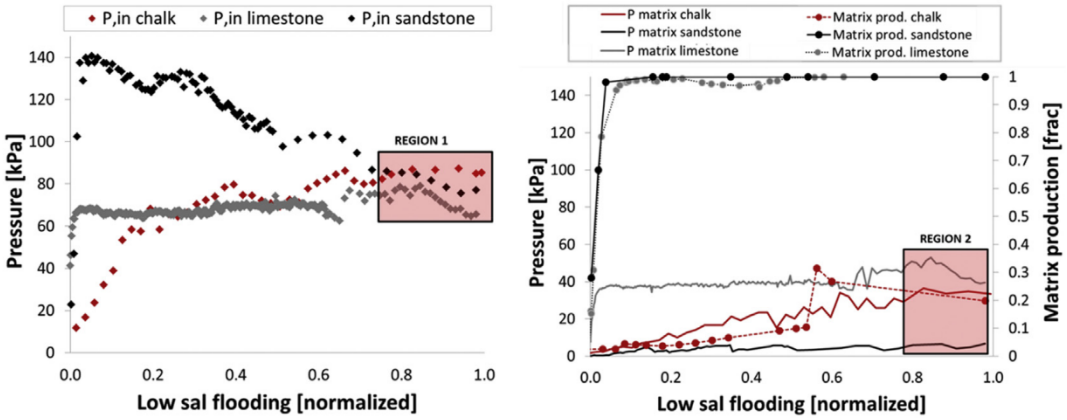

Fig. 4. Left: Injection pressure during low-salinity chase waterflooding of fractured sandstone (Core 4), limestone (Core 5) and chalk (Core 6) core plugs. The inlet pressures varied initially, but collapsed onto the same constant value after significant low-salinity flooding (shown by Region 1). **Right:** The matrix pressures within the core materials varied significantly, with a lower pressure required to flood sandstone compared to limestone and chalk (see Region 2). The limestone and sandstone fractures were completely blocked by gel during low-salinity flooding, while 60% of water flowed through the fracture in the chalk core plug.

expected, the high-permeable sandstone required a lower matrix pressure than the lower-permeability carbonate cores to conduct fluid flow (see "Region 2" in the figure). Further, the fractures through the sandstone and limestone core plugs were completely blocked by gel during low-salinity waterflooding, and all fluids were diverted into and produced through the matrix. In the chalk Core 6, however, 40% of the fluids were produced through the matrix outlets. The remaining 60% of injected fluids were produced through the fracture outlet. This observation, corroborated by the low matrix production flux observed in Core 2 and Core 3, identified an important point; although the gel behaves according to established models, and presumably fills the entire fracture volume during low-salinity floods (when the injection pressure surpasses the originally measured rupture pressure), a low flow capacity in the matrix may cause the gel fracture blocking to be less efficient than expected. The high levels of matrix production observed by Brattekås et al. (2015), where the fractures were completely blocked by gel in most experiments, were not reproduced using low-permeable chalk with residual oil present. The efficiency of the gel to block fractures during waterfloods is thus not only dependent on the gel itself, but strongly dependent on the core material through which the waterflood is taking place.

3.4. Key Observations

Elevated pressure levels were noted during low-salinity flooding compared to high-salinity waterflooding, e.g. shown in Figs. 3 and 4. The following key observations give important implications for further experimental work:

3.4.1. Key observation 1

Similar high pressure values were observed during low-salinity flooding of vastly different core materials, suggesting that the pressure behavior observed was controlled by the gel. The experimental setup, shown in Fig. 1 ***(Left)***, forced all injected fluids into one common inlet for both the matrix halves and the fracture. Thus, injected water must pass through a barrier of gel to reach and flood the matrix during chase-floods. The thickness of the gel barrier determines the pressure drop necessary to pass through it and is given by the volume of gel present in the end pieces. This gel volume was similar in all experiments. The injection pressures measured for Cores 1–6 were therefore controlled by the gel during low-salinity floods. Steps were taken to avoid this effect suring subsequent experiments. Specially designed end pieces, featuring three inlets (one for each matrix half and one for the fracture), were made for use on Core 7.

3.4.2. Key observation 2

Low-salinity waterflooding improves the gel blocking efficiency in all core materials compared to high-salinity waterfloods. In sandstone and limestone core plugs, all injected fluids were produced through the matrix, and fracture flow was completely inhibited by polymer gel. In chalk with residual oil present, water diversion was significantly improved; the amount of water produced through the matrix increased from a low level of <5% up to 40% during low-salinity waterfloods.

3.4.3. Key observation 3

Water diversion improves with water throughput during low-salinity waterfloods. Gel erosion occurs when high-salinity water pass through a ruptured gel network, and gradually opens the fracture to flow, i.e. the gel treatment becomes less efficient with water throughput. In low-salinity waterfloods, although water partly passes through the gel-filled fracture, the opposite effect is observed. Matrix production increases with water throughput, although a portion of the injected water passes through the gel. The mechanism behind improved gel blocking is currently being investigated experimentally, and will offer insight to gel erosion and counteractions during low-salinity chase-floods.

3.4.4. Key observation 4

The improved gel blocking effect during low-salinity waterflooding was not sufficient to completely inhibit fracture flow in chalk with residual oil present. In fully water saturated chalk (Core 1), high-salinity water was diverted into the matrix before gel rupture. Presence of oil increases the resistance to brine flow in the chalk matrix. The low relative permeability to water (k_{rw}) may be comparable to the very low permeability of gel (≈1mD) for some cores, thus the matrix does not necessarily provide the pathway of least resistance for the injected water. It is also possible that water passes through the matrix for some distance, and then channel into the gel-filled fracture to be produced through the fracture outlet. Hence, sweep efficiency is improved by the gel-in-place, but the experimental boundary conditions do not allow this to be distinguished in the experiments. This scenario was previously observed using CT: injected chase water travelled through the matrix for some distance to displace oil, before it entered the gel-filled fracture and was produced through the fracture outlet(Brattekås et al., 2013). Fracture channeling with gel-in-place was in that case explained by the strongly oil-wet preference of the matrix, promoting resistance to water flow at high oil saturations. The pressure available for flow decreases with distance from the inlet, and at some core length the water preferred to flow through the remaining gel-filled fracture to the outlet.

3.5. PET experiments

To avoid the additional pressure drop in the system, caused by a gel

barrier between the injected water and the matrix, specially designed end pieces were used for Core 7. The inlet end piece was separated into two matrix injectors and one fracture injector, shown in Fig. 1 ***(Right)***. Thus, gel was injected into the fracture only, and the matrix end faces were isolated from gel during placement. Positron emission tomography (PET) was used to distinguish the flow paths during waterflooding. To further discuss the effects of low-salinity waterfloods on gel blocking capacity, improved sweep efficiency during waterfloods must be determined for all core lengths, not just close to the outlet (i.e. as determined by material balance from matrix and fracture outlets, respectively).

Gel was injected into a fractured limestone core (Core 7) placed in a small-animal PET-CT scanner. Special end pieces ensured injection of gel into the fracture only, and separate injection of water into the fracture and matrix halves during chase-floods. Water was traced with radioactive pharmaceutical ^{18}F-FDG during high-salinity and following low-salinity chase-floods. PET was used to investigate gel rupture and wormhole formation in a gel-filled fracture during high-salinity waterflooding. The matrix inlets were closed during most of the high-salinity flooding, to accurately test the properties of gel placed in a fracture. Water flow paths (wormholes) through the gel and their evolution during high-salinity flooding can be seen in Fig. 5 and is further elaborated by Brattekås et al. (2016): Gel rupture occurred quickly during high-salinity waterflooding, and one major fluid flow path for water was established at the top of the fracture. By increasing the injection rate, several wormholes were added to the flow path, stretching between the inlet and outlet. The wormhole volume was estimated, and shown to increase with water throughput: after significant waterflooding, wormholes covered 34% of the fracture volume, due to gel erosion. The wormhole width varied significantly within the fracture volume, and directly measured wormhole width by PET was higher than calculated values based on global measurements of pressure and rate. The gel blocking efficiency, reflected by the pressure response during chase-flooding, was high even though wormholes covered a significant part of the fracture: this indicates that gel blocking is controlled by small constrictions (choke points) in the wormholes. This finding also has implications for the mechanism behind improved gel blocking during low-salinity chase waterfloods. The matrix injection ports were opened after significant high-salinity water throughput, during constant rate flooding at 6 ml/h, indicated in Fig. 5 ***(Bottom, Right)***. Water did not enter into the open matrix during late stage high-salinity waterflooding, visible by PET, and fluid flow occurred through the fracture only.

After 24 h of high-salinity waterflooding, without pressure buildup or matrix production, the brine phase was switched to low-salinity water and the waterflood continued. Low-salinity water was injected for 24 h, during which the first 11 h were imaged using PET. Due to the short half-life of ^{18}F-FDG ($t_{1/2}$ = 109 min), new ^{18}F-FDG was produced at a local cyclotron and added to the water phase several times during low-salinity waterflooding. This was necessary to render a radioactive signal high enough to be detected by the PET-scanner. Direct quantification of water saturation development in the matrix and fracture is therefore challenging, but qualitative changes in saturation could be visualized directly by the PET-signal. Fig. 6 shows the development in water saturation during the first 2 h of low-salinity flooding. The core plug and attached fittings (the greyscale image in Fig. 6) is visible by CT, and was used to localize the position of the radioactive PET signal. Water marked by ^{18}F-FDG is visible in blue color on top of the CT image. Water flowed through wormholes in the gel-filled fracture during high-salinity flooding, and Fig. 6 ***(Left)*** shows that the low-salinity water also initially passed through the fracture. One hour into low-salinity waterflooding, Fig. 6 ***(Middle)***, water had entered into and flooded the matrix at the inlet end of the core. After 2 h of low-salinity waterflooding, Fig. 6 ***(Right)***, approximately 30% of the matrix was flooded by low-salinity water. 0.4 pore volumes (PV), i.e. low-salinity water corresponding to 40% of the matrix volume, were injected at this time, suggesting some flow of water through the fracture. Pressure measurements are presented in Fig. 7: no significant increase in pressure was seen during the first 2 h of low-salinity waterflooding, although significant diversion of water to the matrix is visible by PET. This can be explained by the isolation of the matrix during gel placement: in Core 7, contrary to the previous experiments, there is no barrier of low-permeable gel in the inlet end piece, blocking the injected water from flowing into the matrix. Water can therefore pass into the matrix, where its resistance to flow is given by k_{rw}.

Fig. 8 illustrates the water saturation development in Core 7 during the subsequent 8 h of low-salinity waterflooding. At t = 3.3 h, low salinity water has flooded 68% of the core, visible by the blue line in Fig. 8 ***(Top, Left)***, which suggests a completely blocked fracture and fluid flow through the matrix only. Note that the injection pressure (Fig. 7) had not increased significantly at this time. At 5.3 h Fig. 8 ***(Top, Middle)***,

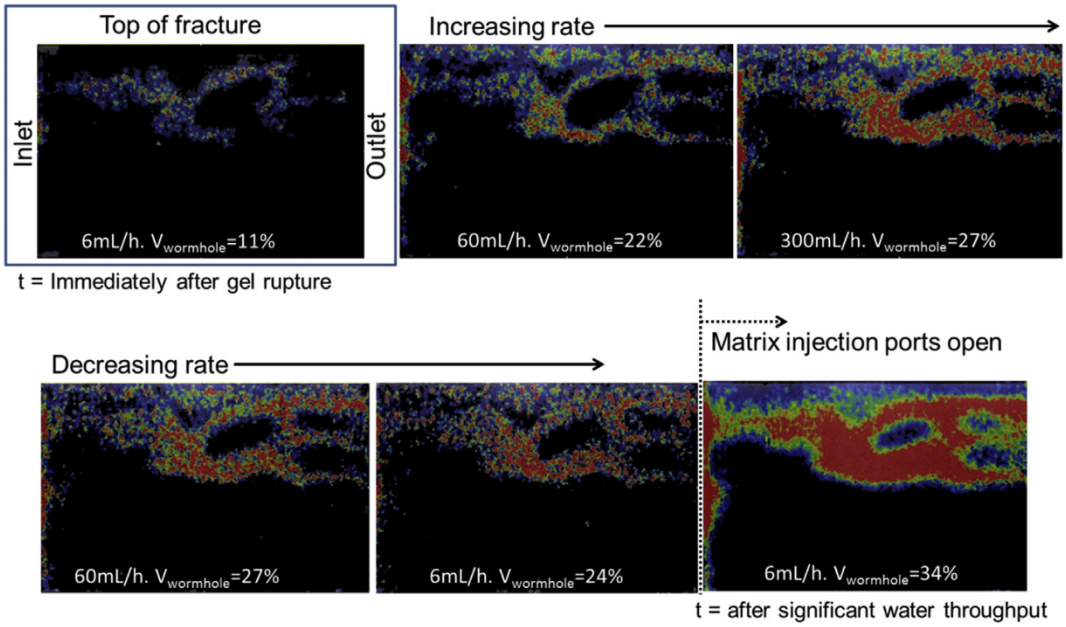

Fig. 5. High-salinity waterflooding of a gel-filled fracture, using radioactive tracer ^{18}F-FDG in the water phase. The colored signal is water passing through gel at different flow rates. Gel rupture occurred (first image) and water passed through the fracture in several non-uniform wormholes. The wormholes expanded with increasing flow rates and water throughput. Figure modified from(Brattekås et al., 2017).

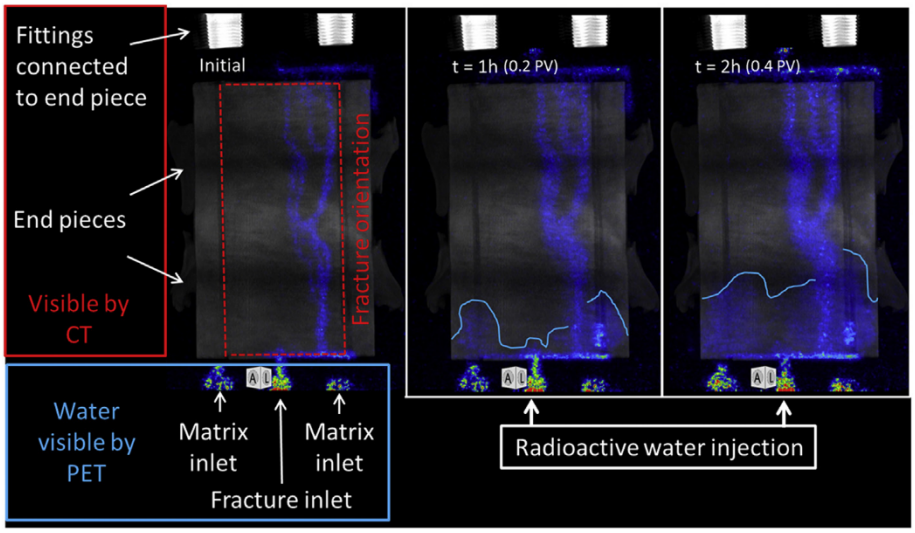

Fig. 6. PET-CT scans for the first 2 h of low-salinity waterflooding. The image to the left shows the initial distribution of fluids. The blue colors is the PET-signal from the radioactive water-phase, initially only present in the fracture. The white and greyscale colors are the CT signal representing the rock core and fittings connected to the end pieces. The core was horizontally aligned during core floods, however; water injection appears upwards in these images. One hour into low-salinity waterflooding (middle image), water has started to enter into the matrix. The blue lines at t = 1 h and t = 2 h indicate the water front position in the matrix, and was added manually to improve visualization.

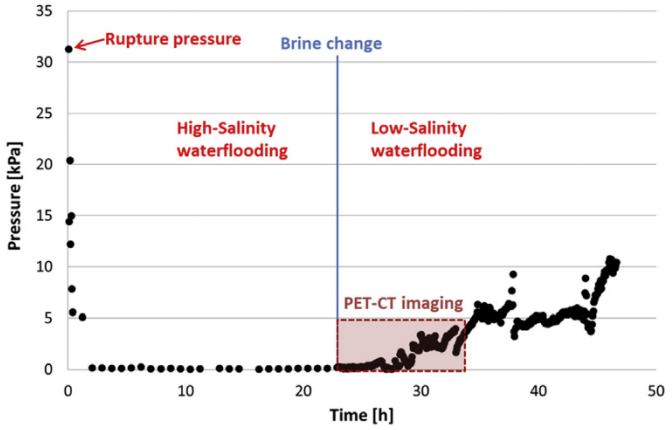

Fig. 7. Pressure development with time during high-salinity and low-salinity waterflooding of Core 6. Note the rupture pressure, denoted close to the y-axis, which is significantly higher than the pressure attained during low-salinity flooding.

water was observed to enter into the core from the outlet end: this is associated with a leak between the matrix and fracture production outlets during gel placement, thus gel was present in the matrix production tubings. The fracture outlet was filled by water due to significant water throughput, and fluids from all three outlets were produced here. As the gel in the fracture becomes stronger due to low-salinity waterflooding, the gel present in the outlet end piece will also experience improved blocking capacity. After being subjected to low-salinity waterflooding for 5.3 h, this gel blocked flow between the matrix and fracture outlet: matrix water was therefore produced into the partially gel-filled matrix production tubings, and an elevated pressure was required to displace gel from the tubing, observed as small-scale disturbances in the differential pressure (Fig. 7). Water was forced into the matrix at the outlet side during pressure buildup, before gel was fully displaced from the production tubings after 7 h of low-salinity waterflooding. The water front did not move further into the matrix from the inlet side during this time period. From 7 to 11 h the low-salinity water saturation continued to increase in the core, and most of the core volume was flooded by low-salinity water when PET-imaging was stopped due to a low radioactive signal. The pressure was approximately 3 kPa at this time, corresponding to 10% of the rupture pressure. This shows that improved gel blocking and diversion of fluids into the matrix can be obtained at pressure values several factors lower than the rupture pressure. Low-salinity flooding of the core continued without imaging. From 13 to 19 h of low-salinity waterflooding, the pressure fluctuated around 5 kPa (one sixth of the initially measured rupture pressure), and the pressure trend was stable. During the last 5 h of waterflooding, the injection pressure increased to 10 kPa, one third of the rupture pressure. Pressure fluctuations were observed when water was diverted into the matrix. This may be caused by an unstable displacement, where some of the water passes through gel-filled or partially gel-filled fracture segments. Parts of the gel network may rupture and be repaired again during low-salinity flooding, causing changing flow patterns through the core.

3.5.1. Wormholes

During high-salinity waterflooding, the wormholes in the fracture were clearly distinguishable and quantifiable by PET. During long-term low-salinity waterflooding the wormholes gradually became visually indistinct, and widespread in the fracture (Fig. 8). The average wormhole width can be calculated from pressure measurements using Poiseuille's law (Brattekås et al., 2017), and is shown in Fig. 9. The calculated average wormhole width from pressure measurements, suggests a decreasing wormhole size to 1% of the original size. Calculated wormhole values do not represent the real spread of the wormholes in a fracture (Brattekås et al., 2016). However; a reduced calculated wormhole width indicates that a decreased radioactive signal in the fracture should be expected. It remains unclear whether the indistinct wormholes, visualized by PET, were descriptive of the gel behavior during flooding, and we suspect that diffusion of radioactive water into the gel may have occurred during long-term waterflooding. Very few references on diffusion in PET-experiments are found in the literature, and diffusion will be further investigated and quantified in future work. A radioactive pharmaceutical with a longer half-life may be used, to closely monitor and define the mechanism behind improved fracture blocking during low-salinity flooding.

3.6. Implications for use of low-salinity chase-floods to improve gel treatments

Brattekås et al. (2016) reported for the first time significant improvement in gel blocking ability during low salinity waterflooding of

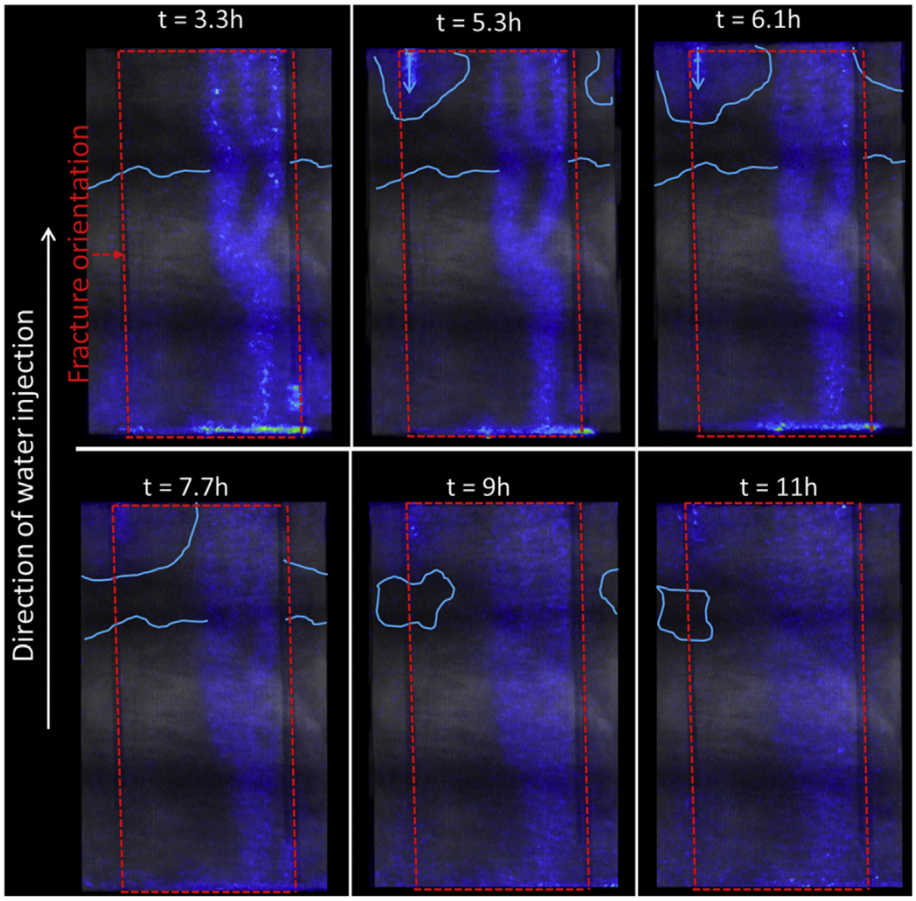

Fig. 8. PET-CT scans for the subsequent 8 h of low-salinity waterflooding. The end piece and fittings are removed from the images, and only the matrix halves and fracture is visible. The water front moved further into the matrix with time, indicating a blocked or partially blocked fracture.

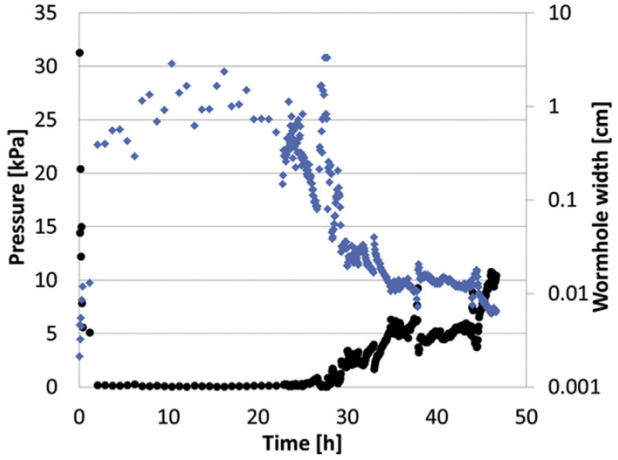

Fig. 9. Calculated wormhole size based on pressure measurements during high-salinity and low-salinity waterflooding.

fractured cores, caused by salinity differences between the gel solvent and injected water phase, and stated: "We believe that, during field operations with proper zone isolation, pressure gradients during chase-flooding will be controlled mainly by the matrix flow capacity and not dictated by the gel as observed in these experiments, as long as the injection pressure is below the gel rupture pressure." This has been confirmed in the Core 7 experiment, where the matrix was isolated from gel during placement: low-salinity chase-flooding improved the fracture blocking, and most of the matrix flooded at a pressure a factor ten lower than the rupture pressure. Integrated EOR (iEOR) with polymer gel conformance control and low-salinity chase-floods shows promise for future application. Gel swelling is the most likely cause for improved blocking. However, it remains unclear whether the gel swells uniformly to constrict wormholes, or if gel particles dislodge from the filter-cake, swell and clog in narrow parts of the wormholes. PET imaging was used to investigate changing wormholes during flow, and was efficient during high-salinity waterfloods, where the changes occur on a short time scale (minutes to hours). During low-salinity waterfloods (hours to days), the experimental setup must be altered and the challenge of diffusion resolved to accurately determine the mechanism behind improved blocking. Current work involves the use of several *in-situ* imaging methods for this purpose.

4. Conclusions

- Gel blocking ability during chase waterfloods depends on the salinity of the chase water.
  - **Chase-flood by water with salinity equal to that of the gel solvent**: the matrix flow rate may be high until the gel ruptures, after which the fracture blocking efficiency of gel decreases with water throughput. The high initial pressure response of the gel was not restored.
  - **Chase-flood by low-salinity water**: gel fracture blocking was improved when the chase water salinity was reduced with respect to the gel solvent, and fluids were diverted into the matrix. Gel fracture blocking efficiency increased with low-salinity water throughput.
- Gel blocking ability during chase waterfloods depends on the core material through which the waterflood is taking place.

  - Matrix production was, as expected, controlled by the core material that water must pass through during chase-floods, requiring a higher pressure to flood low-permeable core material.
  - The presence of residual oil influenced the ease with which water flows through the porous rock. Low-salinity waterfloods did not completely inhibit fracture flow in chalk with residual oil present.
  - Water was diverted into the matrix for all ranges of permeability: sandstone and low-permeable carbonates
- The high pressures measured during low-salinity waterfloods through one common inlet (in some cases higher than the rupture pressure) were controlled by the gel volume present in the inlet end pieces.
- Changing the experimental boundary conditions, by separating matrix and fracture injection points, showed that low-salinity water may enter and flood the matrix at pressures significantly lower than the rupture pressure. Imaging by PET showed improved gel blocking and fluid diversion into the matrix without an increase in pressure, and most of the matrix was flooded by low-salinity water at a pressure a factor ten lower than the rupture pressure.

Acknowledgements

The corresponding author acknowledge the Research Council of Norway and the industry partners; ConocoPhillips Skandinavia AS, Aker BP ASA, Eni Norge AS, Maersk Oil Norway AS, DONG Energy A/S (Denmark), Statoil Petroleum AS, ENGIE E&P NORGE AS, Lundin Norway AS, Halliburton AS, Schlumberger Norge AS, Wintershall Norge AS of the National IOR Centre of Norway for support.

The PET imaging was performed at the Molecular Imaging Center, Dept. of Biomedicine at the University of Bergen.

References

Aalaie, J., Rahmatpour, A., Vasheghani-Farahani, E., 2009. Rheological and swelling behavior of semi-interpentrating networks of polyacrylamide and scleroglucan. Polym. Adv. Technol. 20, 1102–1106. https://doi.org/10.1002/pat.1369.

Bai, B.J., Li, L.X., Liu, Y.Z., Liu, H., Wang, Z.G., You, C.M., 2007. Preformed particle gel for conformance control: factors affecting its properties and applications. SPE Reserv. Eval. Eng. 10 (4), 415–422. https://doi.org/10.2118/89389-Pa.

Brattekås, B., Graue, A., Seright, R., 2016. Low-salinity chase waterfloods improve performance of Cr(III)-acetate hydrolyzed polyacrylamide gel in fractured cores. SPE Reserv. Eval. Eng. 19 (02), 331–339. https://doi.org/10.2118/173749-PA.

Brattekås, B., Haugen, Å., Ersland, G., Eide, Ø., Graue, A., Fernø, M.A., 2013. Fracture mobility control by polymer gel- integrated EOR in fractured, oil-wet carbonate rocks. In: Paper Presented at the EAGE Annual Conference & Exhibition Incorporating SPE. Europec, London, UK.

Brattekås, B., Haugen, Å., Graue, A., Seright, R.S., 2014. Gel dehydration by spontaneous imbibition of brine from aged polymer gel. SPE J. 19 (01), 122–134. https://doi.org/10.2118/153118-PA.

Brattekås, B., Pedersen, S.G., Nistov, H.T., Haugen, A., Graue, A., Liang, J.-T., Seright, R., 2015. Washout of Cr(III)-acetate-HPAM gels from fractures: effect of gel state during placement. SPE Prod. Operations 30 (02), 99–109. https://doi.org/10.2118/169064-PA.

Brattekås, B., Steinsbø, M., Graue, A., Fernø, M.A., Espedal, H., Seright, R.S., 2017. New insight into wormhole formation in polymer gel during water chase floods with positron emission tomography. SPE J. 22 (01), 32–40. https://doi.org/10.2118/180051-PA.

Ekdale, A.A., Bromley, R.G., 1993. Trace fossils and ichnofabric in the Kjølby gaard marl, uppermost creataceous. Den. Bull. Geol. Soc. Den. 31, 107–119.

Ganguly, S., Willhite, G.P., Green, D.W., McCool, C.S., 2002. The effect of fluid leakoff on gel placement and gel stability in fractures. SPE J. 7 (03), 309–315. https://doi.org/10.2118/79402-PA.

Horkay, F., Tasaki, I., Basser, P.J., 2000. Osmotic swelling of polyacrylate hydrogels in physiological salt solutions. Biomacromolecules 1, 84–90. https://doi.org/10.1021/bm9905031.

Klein, E., Reuschle, T., 2003. A model for the mechanical behaviour of bentheim sandstone. Pure Appl. Geophys. 160, 833–849.

Liang, J.-T., Lee, R.L., Seright, R.S., 1993. Gel placement in production wells. SPE Prod. Facil. 8 (November), 276–284.

Morrow, N., Buckley, J., 2011. Improved oil recovery by low-salinity waterflooding. J. Pet. Technol. 63 (05), 106–112. https://doi.org/10.2118/129421-JPT.

Riskedal, H., Tipura, L., Howard, J., Graue, A., 2008, Oct 29.- Nov 2.. NMR Monitoring of Spontaneous Brine Imbibition in Carbonates. Paper presented at the Society of Core Analysts, Abu Dhabi.

Romero-Zeron, L.B., Hum, F.M., Kantzas, A., 2008. Characterization of crosslinked gel kinetics and gel strength by use of NMR. SPE Reserv. Eval. Eng. 11 (03), 439–453. https://doi.org/10.2118/86548-PA.

Seright, R.S., 2001. Gel propagation through fractures. SPE Prod. Operations 16 (4), 225–231. https://doi.org/10.2118/74602-pa.

Seright, R.S., 2003a. An alternative view of filter-cake formation in fractures inspired by Cr(III)-acetate-HPAM gel extrusion. SPE Prod. Facil. 18 (1), 65–72.

Seright, R.S., 2003b. Washout of Cr(III)-acetate-HPAM gels from fractures. In: Paper Presented at the International Symposium on Oilfield Chemistry, Houston, TX.

Seright, R.S., Martin, F.D., 1993. Impact of gelation Ph, rock permeability, and lithology on the performance of a monomer-based gel. SPE Reserv. Eng. 8 (1), 43–50.

Tie, H., 2006. Oil Recovery by Spontaneous Imbibition and Viscous Displacement from Mixed-wet Carbonates. PhD thesis. The University of Wyoming, Laramie, Wyoming.

Tu, T.N., Wisup, B., 2011. Investigating the effect of polymer gels swelling phenomenon under reservoir conditions on polymer conformance control process. In: Paper Presented at the International Petroleum Technology Conference, Bangkok, Thailand.

Viksund, B.G., Morrow, N.R., Ma, S., Graue, A., 1998. Initial water saturation and oil recovery from chalk and sandstone by spontaneous imbibition. In: Paper Presented at the Inlt. Symposium of Soc. Of Core Analysts, the Hague.

Wilton, R., Asghari, K., 2007. Improving gel performance in fractures: chromium pre-flush and overload. J. Can. Petroleum Technol. 46 (02) https://doi.org/10.2118/07-02-04.

Witherspoon, P.A., Wang, J.S.Y., Iwai, K., Gale, J.E., 1980. Validity of cubic law for fluid flow in a deformable rock fracture. Water Resour. Res. 16 (6), 1016–1024. https://doi.org/10.1029/WR016i006p01016.

Zhang, H., Bai, B., 2011. Preformed-particle-gel transport through open fractures and its effect on water flow. SPE J. 16 (2), 388–400. https://doi.org/10.2118/129908-PA.